ELSEVIER

Journal of Power Sources 62 (1996) 223–227

JOURNAL OF POWER SOURCES

Short Communication

Research of Zn–Mn spinel electrode material for aqueous secondary batteries [1]

Yang Hui, Yang Huaquan, Lu Yinlin, Li Neng, Li Bingxiong

Department of Chemistry, Peking University Beijing, Beijing, 100871 People's Republic of China

Received 14 February 1996; accepted 13 March 1996

Abstract

Zn–Mn complex oxides have been prepared by the organic acid complex method. X-ray diffraction (XRD) analyses show that the major product is a Zn–Mn spinel phase. The capacity of the sample is above 200 mAh g^{-1} on cycling in aqueous LiOH electrolyte, but deep-discharge has great influence on the cycling property of the sample. XRD analysis shows that Li^+ ions are intercalated into and extracted from the Zn–Mn spinel lattice during the discharge and charge process.

Keywords: Zinc–manganese spinel; Secondary batteries; Lithium intercalation; Cathode materials

1. Introduction

Zn/MnO_2 primary batteries have been used for many years. But there has been much less development of Zn–Mn secondary batteries. Poor cycling performance is the main problem for rechargeable Zn/MnO_2 batteries [1]. A rechargeable battery of $Zn/ZnSO_4/Zn_xMn_{3-x}O_4$ ($x=0.01$–1.0) has been developed [2]. The lithium insertion reaction of $ZnMn_2O_4$ has been studied in non-aqueous electrolytes [3], but there have been no investigations in aqueous electrolytes.

In this work, the citric acid complex method is used to prepare Zn–Mn complex oxides. The samples are employed as cathode active material in aqueous LiOH cells and the cycle performance is determined. The electrochemical properties of the samples are characterized by a.c. impedance and cyclic voltammetric measurements. The intercalation and extraction of Li^+ ions into the Zn–Mn spinel lattice in aqueous LiOH solution during the cycle are demonstrated by X-ray diffraction (XRD).

2. Experimental

The Zn–Mn complex oxides were prepared by the citric acid complex method. $Zn(NO_3)_2$ and $Mn(NO_3)_2$ solutions were mixed at given Zn:Mn ratios (Zn:Mn = 1:2, 0.9:2, 0.8:2, 0.7:2, 0.6:2, 0.5:2, 0.4:2). The citric acid was added at ratios of Zn:acid = 1:1, Mn:acid = 1:1. The mixture was evaporated in air and a grey-black solid was obtained. The resulting samples were ground and activated at 250 °C for 2 h in air, they were then heated at 400, 600, 800 °C for 2 h, respectively, and the final products were obtained.

Powder XRD analyses were performed using an automated Rigaku diffractometer with Cu Kα radiation.

The cycling performance of the cathode material was evaluated in laboratory cells that comprised: Zn/saturated LiOH aqueous solution (saturated with ZnO)/$ZnMn_2O_4$ + graphite.

The cathode consisted of 0.2 g of sample (for example, $ZnMn_2O_4$), 0.8 g of graphite, and 0.08 g of polytetrafluoroethylene (PTFE) powder as a binder. The mixture was pressed onto a nickel screen at 20 MPa. The cells were cycled at a current density of 1 mA cm^{-2}.

A Solatron 1250 frequency response analyser was used to perform a.c. impedance measurements. The results were represented in electrical conductivities. Samples of 0.2 g pressed into a disc at 14 MPa for 1 min were used.

For cyclic voltammetric (CV) experiments, a three-electrode cell was used. The working electrode consisted of the sample with graphite powder. Zinc foil was used as a counter electrode, and a Hg/HgO electrode served as a reference electrode (for $ZnSO_4$ electrolyte, the reference electrode was a saturated calomel (SCE) electrode). The electrolyte was the same as that used in cycling performance tests. The scan rate was 1 mV s^{-1}.

[1] This work was supported by Chinese National Nature Science Foundation.

PII S0378-7753(96)02416-0

3. Results and discussion

The compositions of the samples as determined by XRD analyses, are shown in Table 1. The major product was Zn–Mn spinel ($Zn_yMn_{3-y}O_4$). For samples with Zn:Mn ratios from 0.5:2 to 1:2, the composition is similar. The XRD patterns of samples with Zn:Mn ratios of 0.5:2 and 1:2 are given in Fig. 1. Data for only 250 °C and 600 °C samples are shown (the 400 °C sample is similar to the 250 °C sample, the 800 °C sample is similar to 600 °C sample). At low temperature (250, 400°C), the samples are composed of $Zn_{0.5}Mn_{2.5}O_4$ and a small amount of ZnO. The amount of ZnO decreases when the Zn:Mn ratio is decreased from 1:2 to 0.5:2. For the samples with a Zn:Mn ratio of 0.4:2, the low-temperature product is pure Zn–Mn spinel ($Zn_{0.5}Mn_{2.5}O_4$) without ZnO (see Fig. 2). At high temperature (600, 800 °C), the samples with ratios from 0.5:2 to 1:2 yield pure Zn–Mn spinel ($Zn_yMn_{3-y}O_4$) (see Fig. 1), while the samples with Zn:Mn = 0.4:2 are composed of $Zn_yMn_{3-y}O_4$ and a large amount of α-Mn_2O_3 (see Fig. 2).

The electrical conductivities of the samples are given in Table 2. The conductivities decrease from 250 to 400 °C and from 600 to 800 °C, respectively. This can be attributed to the more perfect structure at higher temperature (400 °C for low temperature and 800 °C for high temperature). The electrical conductivities are poor (10^{-8} to $5\times10^{-7}\ \Omega^{-1}\,cm^{-1}$). Thus, a large amount of graphite must be added to the samples while making electrodes in order to improve the conductivity.

Table 1
Composition of samples determined by XRD analysis

Zn:Mn = x:2	Temperature (°C)	Composition
$0.5 \le x \le 1$	250, 400, 600, 800	$Zn_{0.5}Mn_{2.5}O_4$ + ZnO $Zn_yMn_{3-y}O_4$ (y = 0.6–1)
$x = 0.4$	250, 350 600, 800	$Zn_{0.5}Mn_{2.5}O_4$ $Zn_yMn_{3-y}O_4 + Mn_2O_3$

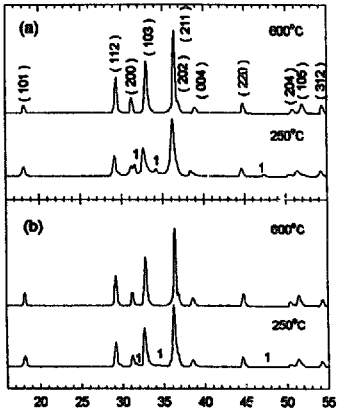

Fig. 1. X-ray diffraction profiles of samples: (a) Zn:Mn = 1:2; (b) Zn:Mn = 0.5:2. Peaks labelled 1 are from ZnO. Others are from $Zn_yMn_{3-y}O_4$.

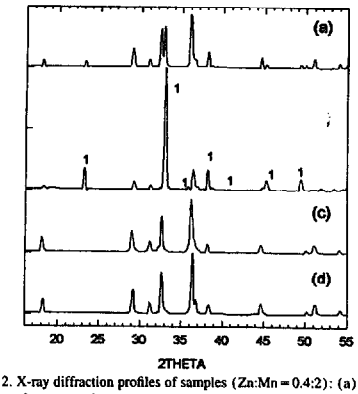

Fig. 2. X-ray diffraction profiles of samples (Zn:Mn = 0.4:2): (a) 800 °C; (b) 600 °C; (c) 350 °C, and (d) 250 °C. Peaks labelled 1 are from α-Mn_2O_3. Others are from Zn–Mn spinel ($Zn_yMn_{3-y}O_4$).

Typical discharge curves for $ZnMn_2O_4$ (Zn:Mn = 1:2, 800 °C) are shown in Fig. 3. The first discharge has poor capacity. After deep-discharge, however, the capacity is improved. This can be observed from the second and following discharges. A discharge plateau at about 0.9 V is also observed. Since 0.9 V is used as the end voltage to calculate the capacity,

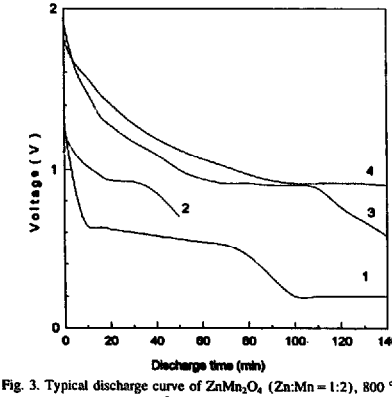

Fig. 3. Typical discharge curve of $ZnMn_2O_4$ (Zn:Mn = 1:2), 800 °C at a current density of 2 mA cm^{-2} for a cell of Zn/LiOH/$ZnMn_2O_4$. Curves (1) to (4) refer to the first to fourth discharges, respectively.

Table 2
Electrical conductivity of samples ($\times 10^{-8}\ \Omega^{-1}\ cm^{-1}$)

	250 °C	400 °C	600 °C	800 °C
Zn:Mn = 1.0:2	20.0	5.6	6.4	1.4
Zn:Mn = 0.9:2	14.0	1.2	46.0	3.8
Zn:Mn = 0.8:2	20.0	1.8	4.4	1.5
Zn:Mn = 0.7:2	20.0	4.4	8.4	2.3
Zn:Mn = 0.6:2	15.0	2.5	28.0	1.3
Zn:Mn = 0.5:2	9.2	1.9	4.4	2.5
Zn:Mn = 0.4:2	2.0	1.7[a]	27.0	3.0

[a] This sample was synthesized at 350 °C.

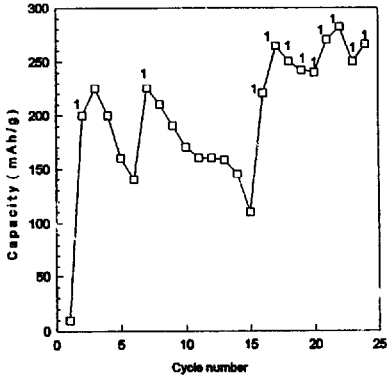

Fig. 4. Capacity of $Zn_{0.5}Mn_{2.5}O_4$. Points labelled 1 are those after deep discharge. Others are not deep-discharged.

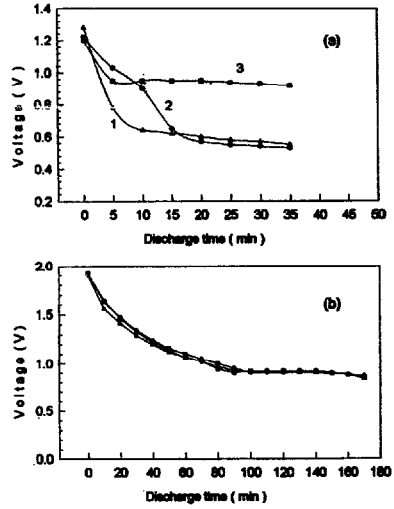

Fig. 5. Discharge curves: (a) first discharge, and (b) after deep discharge. Curves (1) $ZnMn_2O_4$: 0.1 g, (2) $Zn_{0.5}Mn_{2.5}O_4$: 0.2 g, and (3) $Zn_yMn_{3-y}O_4Mn_2O_3$: (Zn:Mn = 0.4:2, 800 °C) 0.2 g.

the capacity may change greatly (see Fig. 4) while the plateau changes only a little.

The influence of deep-discharge on capacity is shown in Fig. 4. The initial poor capacity can be improved only after a deep-discharge, and if it is always deep-discharged, the cathode material can be kept at a high specify capacity (above 200 mAh g^{-1}). By contrast, the capacity falls when deep-discharge is stopped.

Samples of different compositions differ in their first discharges (see Fig. 5(a)), the discharge plateau of 0.95 V for sample 3 is attributed to Mn_2O_3. The cycle performance tends to be the same after deep-discharge (see Fig. 5(b)).

Cyclic voltammograms for different samples are shown in Fig. 6. The scan range is from 0.6 to −1.3 V, which is similar to the charge/discharge voltage range of the cells used in cycle performance tests. The first scan begins at about 0 V and the negative-going scan is carried out first. The first reductive process differs with different samples, while the following oxidative and reductive processes are similar. The results of Fig. 6 are similar to those of $LiMn_2O_4$ in LiOH aqueous solution. The peaks at −0.7 and +0.1 V refer to the reductive process (Li^+ insertion) and the oxidative process (Li^+ extraction), respectively. The peaks at −1.3 and +0.6 V represent the processes of H_2 and O_2 evolution, respectively.

Tests performed on the $Zn/ZnSO_4/Zn_{0.5}Mn_{2.5}O_4$ cell showed that the system differs from LiOH systems. The cyclic voltammogram for $Zn/Zn_{0.5}Mn_{2.5}O_4$ in $ZnSO_4$ electrolyte is shown in Fig. 7. The peaks at −1.2 and +0.8 V indicate the formation of H_2 and O_2. No other anodic peaks are observed at the same scan rate, so the mechanism of $Zn_{0.5}Mn_{2.5}O_4$ in $ZnSO_4$ is different from that in LiOH.

The XRD patterns of samples ($Zn_{0.5}Mn_{2.5}O_4$) before and after discharge and charge are given in Fig. 8. After discharge, a diffraction peak appears near 18.7° and its relative intensity

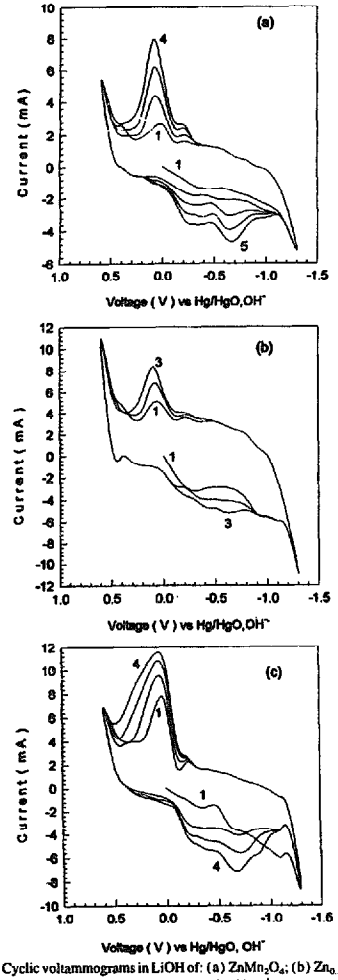

Fig. 6. Cyclic voltammograms in LiOH of: (a) $ZnMn_2O_4$; (b) $Zn_{0.5}Mn_{2.5}O_4$, and (c) $Zn_yMn_{3-y}O_4 + Mn_2O_3$; scan rate = 1 mV s^{-1}.

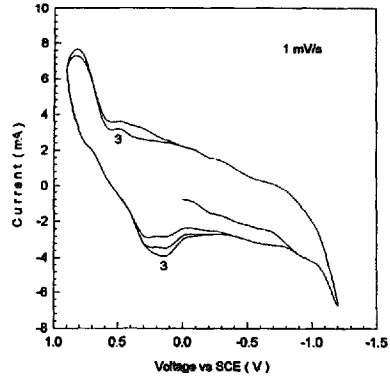

Fig. 7. Cyclic voltammogram of $Zn_{0.5}Mn_{2.5}O_4$ in 2 M $ZnSO_4$.

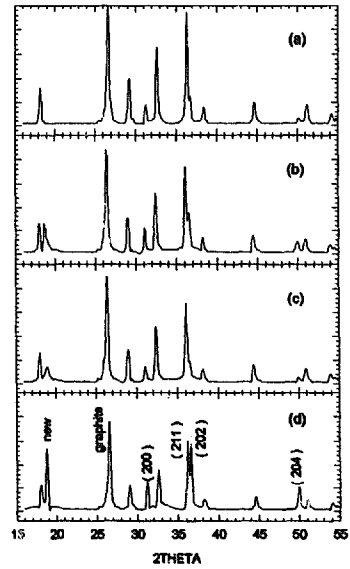

Fig. 8. XRD patterns of $Zn_{0.5}Mn_{2.5}O_4$ (a) before discharge, (b) after third discharge; (c) after third charge, and (d) after eighth discharge.

increases with increase in cycle number. Additionally, the relative intensities of the 200, 202, 204 peaks of the Zn–Mn spinel increase greatly while those of the other peaks of the Zn–Mn spinel shows little change. Since the 18.7° diffraction peak is the characteristic peak of $LiMn_2O_4$ and the abnormal increase of the 200, 202, 204 peaks can be attributed to the insertion of Li^+ ions and the formation of $LiMn_2O_4$, it is concluded that Li^+ ions intercalated into the lattice of the Zn–Mn spinel during the discharge. The XRD patterns of the samples after the third discharge and the third charge clearly show that the initial structure can be only partly restored after cycling. Some irreversible reaction must occur when the cell is discharged.

4. Conclusions

For Zn–Mn complex oxides obtained by the organic acid method, the major products are Zn–Mn spinel ($Zn_yMn_{3-y}O_4$). It is found that $ZnSO_4$ is not suitable for rechargeable $Zn/Zn_yMn_{3-y}O_4$ batteries. The samples are used as positive-plate materials in an aqueous LiOH secondary cell and give a specific capacity of up to 200 mAh g^{-1}. Deep-discharge exerts a great influence on the cycle performance of the cell. XRD analyses show that Li^+ ions intercalates into and extract from the Zn–Mn spinel lattice during the respective discharge and charge process.

References

[1] Y.F. Yao, N. Gopta and H.S. Wroblowa, *J. Electrochem. Soc.*, *223* (1987) 107.

[2] T. Kenichi, S. Hajime, S. Takayaki and i. Masanori, *Jpn. Patent No. 03 112 068 [91 112 068]*.

[3] C.J. Chen, M. Greenblatt and J.V. Waszczar, *Mater. Res. Bull.*, *21* (1986) 609.